



UNIVERSITY OF LEEDS

This is a repository copy of *Crystallisation of copper sulphate pentahydrate from aqueous solution in absence and presence of sodium chloride*.

White Rose Research Online URL for this paper:

<http://eprints.whiterose.ac.uk/151850/>

Version: Accepted Version

Article:

Justel, FJ, Camacho, DM, Taboada, ME et al. (1 more author) (2019) Crystallisation of copper sulphate pentahydrate from aqueous solution in absence and presence of sodium chloride. *Journal of Crystal Growth*, 525. 125204. ISSN 0022-0248

<https://doi.org/10.1016/j.jcrysGro.2019.125204>

© 2019, Elsevier. This manuscript version is made available under the CC-BY-NC-ND 4.0 license <http://creativecommons.org/licenses/by-nc-nd/4.0/>.

Reuse

This article is distributed under the terms of the Creative Commons Attribution-NonCommercial-NoDerivs (CC BY-NC-ND) licence. This licence only allows you to download this work and share it with others as long as you credit the authors, but you can't change the article in any way or use it commercially. More information and the full terms of the licence here: <https://creativecommons.org/licenses/>

Takedown

If you consider content in White Rose Research Online to be in breach of UK law, please notify us by emailing eprints@whiterose.ac.uk including the URL of the record and the reason for the withdrawal request.

CRYSTALLISATION OF COPPER SULPHATE PENTAHYDRATE FROM AQUEOUS SOLUTION IN ABSENCE AND PRESENCE OF SODIUM CHLORIDE

F.J. Justel^{1*}, D.M. Camacho², M.E. Taboada¹, and K. J. Roberts²

¹Department of Chemical Engineering and Mineral Processing, University of Antofagasta,
Antofagasta, Chile

²School of Chemical and Process Engineering, University of Leeds, Leeds, LS2 9JT, United
Kingdom

Abstract

The recrystallization of copper sulphate from aqueous solution represents an important unit operation in copper mining and recovery and there is significant current interest, on environmental grounds, to the use of sea water as an alternative solution. Hence, the effect of sodium chloride on the shape, size, composition and growth kinetics of copper sulphate pentahydrate crystals is assessed and compared with results in freshwater in order to understand the effect of the principal ions present in brine (Na^+ and Cl^-) on the crystallisation process. The cooling rate and sodium chloride concentration are observed to have an effect in the crystal shape and size of the copper sulphate crystals albeit the purity of crystals is not significantly affected by the sodium chloride concentration used. Analysis of the crystal growth kinetics of copper sulphate in the supersaturation range from 0.682 to 0.787, and from 0.348 to 0.458 in aqueous and brine solvent, respectively, reveals a significant dependence

on the growth environment, in which the growth of the {1-10} and {1-1-1} faces of crystals grown in aqueous solutions is consistent with the power law and BCF mechanisms (R^2 of 99.5% and 96%, respectively). In contrast for crystals grown in brine the results suggest that both the {1-10} and {1-1-1} faces grow via the BCF mechanism (R^2 of 99.5% and 96%, respectively). This difference in the face-specific growth mechanisms, in the different crystallisation media, is evidenced in the crystal shape revealing slightly more elongated crystals in aqueous solutions.

Keywords: A1. Copper sulphate, A2. Sodium Chloride, B1. Crystal Growth Kinetics Mechanism, C1. Industrial Crystallisation

1. Introduction

Copper sulphate pentahydrate is an important industrial compound related to copper mining due to its wide range of commercial uses [1-3]. In Chile, some mining companies crystallise this salt from hydrometallurgical processes using freshwater, where copper is obtained from ores containing oxidised copper minerals [4]. However, in order to be able to minimize the use of freshwater in the crystallisation process, seawater is now being increasingly used for the crystallisation of copper sulphate pentahydrate and thus the impact of this needs to be assessed [5].

Copper sulphate pentahydrate ($\text{CuSO}_4 \cdot 5\text{H}_2\text{O}$), also referred to as bluestone and blue vitriol, is found in nature as the mineral chalcanthite [3]. It belongs to the triclinic crystal system crystallising in space group P1 with unit-cell parameters: $a = 6.1224 (4) \text{ \AA}$; $b = 10.7223 (4) \text{ \AA}$; $c = 5.9681 \text{ \AA}$; $\alpha = 82.35 (2)^\circ$; $\beta = 107.33 (2)^\circ$; $\gamma = 102.60 (4)^\circ$; $V = 364.02 (3) \text{ \AA}^3$; $Z = 2$; $D = 2.278 \text{ g/cm}^3$. Figure 1 shows the crystal habit of copper sulphate pentahydrate crystals which is a combination of pinacoids [6].

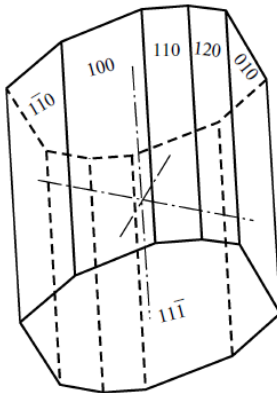


Figure 1. Habit of $\text{CuSO}_4 \cdot 5\text{H}_2\text{O}$ crystal [6].

Copper sulphate pentahydrate crystallisation studies using freshwater have been carried out by several authors: Ishii and Fujita [7], examined the stability of copper sulphate aqueous solutions at the first supersaturation concentration, in a batchwise stirred reactor, using different temperatures and stirring rates. Zumstein and Rousseau [8] focused their work on the agglomerate formation during the batch and continuous copper sulphate crystallisation. Giulietti et al. [1, 9, 10], characterized the copper sulphate pentahydrate crystallisation from batch cooling experiments and studied the effect of additives on the crystallisation process. Manomenova et al. [6] developed a technique for growing large single crystals for application as optical filters, analysing the transmission spectra, their associated impurities, thermal stability and crystal structure.

However, little information is available in the literature regarding the effect of seawater as a recrystallisation solvent upon the resultant physical chemical processes of the copper sulphate crystals [11-14]. Some of these studies have represented the solid-liquid equilibrium of copper sulphate-sulphuric acid-seawater systems by means of a methodology that uses the Pitzer and the Born model [15-16] to quantify the relative impact of copper sulphate and sulphuric acid, respectively, on the phase diagram.

The impact of sodium chloride on crystallisation processes in general has been studied previously: Brandse et al. [17], studied the effect of NaCl on the growth kinetics of calcium sulphate dehydrate and Sheikholeslami and Ong [18] examined the salinity effect on the CaCO_3 and CaSO_4 crystallisation, where different NaCl concentrations were used to study the crystal structure and size, amongst others.

The growth rate of each crystallographically unique crystal form {hkl} is different depending on growth environmental factors such as supersaturation, temperature, solvents, and impurities. The most common methods for the measurement of the growth rate of crystals [19] are the measurement of the linear growth rate on specific faces of a single crystal or by estimating an overall linear growth rate from the mass deposition rates on the bulk mass of a large number of crystals. The single crystal measurement method avoids the impact of other heterogeneous physical phenomena such as the collision of crystals with other objects, e.g. the wall of the vessel or other crystals that may have an effect on the overall growth kinetics [20]. Previous studies have been carried out on a number of ionic compounds including the measurement of the growth rates of ammonium and potassium dihydrogen phosphate crystal faces under controlled conditions of temperature, supersaturation, and solution velocity [21]; Davey and Mullin [22] studied the effect of ionic species on the growth kinetics and impurity incorporation for the {101} and {100} faces of ammonium dihydrogen phosphate single crystals; Sweegers et al. [23] used in-situ optical microscopy to measure the growth rates of individual {001}, {110}, and {100} faces for different types of gibbsite crystals as a function of the driving force; Suharso [24] reported the growth mechanism for sodium borate tetrahydrate (borax) single crystals for the {111} habit planes at various relative supersaturations using in situ optical microscopy.

Given the lack of detailed studies on the growth kinetics of copper sulphate pentahydrate, it is the aim of this study to deliver fundamental information on the morphology and crystal growth kinetics of copper sulphate pentahydrate as a function of the solution environment (aqueous or brine solvents). These experimental data were collected using a methodology previously developed for the analysis of Ibuprofen single crystal growth [25], while the

subsequent analysis of crystal growth kinetics was carried out using models which consider the effect in series of mass transfer and integration of growth units to the crystal surface derived elsewhere [26,27].

Critically this work seeks to understand the effect of the principal ions from seawater in the overall crystallisation process. This knowledge will allow us to obtain valuable information that could be useful in the design of the copper sulphate crystallisation process using seawater. In all the experiments, a sodium chloride concentration of 2.4 wt % was used in order to simulate the natural seawater system reported by Hernández et al. [11] and Justel et al. [12]. The analysis comprises the cooling crystallisation experiments to visualize changes in the crystals size and shape in each media, followed by the assessment of crystals' single faces growth kinetics for the determination of the growth mechanisms in different media.

2. Materials and Methods

2.1 Materials

The reagents used in this work were of analytical grade: Copper sulphate pentahydrate, Merck, 99%; sodium chloride, Merck, 99.5%, and distilled deionized water ($0.054 \mu S \cdot cm^{-1}$). No further purification of these materials was carried out.

2.2 Equipment and experimental procedure

2.2.1 Crystallisation experiments

Crystallisation experiments were carried out using the Technobis Crystalline® system (see: <https://www.crystallizationsystems.com/Crystalline>). This facilitates 8 parallel reactors and can hold up to 8 standard disposable glass vials (O 16.6 mm, flat bottomed, 8 mL). Each reactor can be independently loaded, programmed, and operated. The temperature range can be varied from -15 to 150 °C and stirring rates between 0 to 1250 rpm are available using magnetic and/or overhead agitators. This platform provides an inlet for a dry purge gas (typically nitrogen) to prevent condensation on the reactor blocks and electronics. This system incorporates high quality digital video imaging system for each reactor. These can be synchronised with the turbidity measurements and temperature profile of each independent reactor. Data was collected using “particle viewer” mode through which both the reactor temperature and on-line particle image data was recorded.

In-situ batch cooling crystallisation experiments were performed for copper sulphate solutions at the concentration of 29.52 wt %, in absence and in presence of 2.4 wt % of sodium chloride, to visualize the crystallisation at an early stage. The solutions were subject to heating and cooling cycles, with each cycle initiated by heating the solutions up to 70°C where they were held for an hour to ensure complete homogenization and then cooled to 0°C where they were also held for an hour to allow equilibration. This temperature profile was applied using four different cooling rates 2.0, 1.0, 0.5, and 0.3 °C/min for both the CuSO₄ + H₂O and CuSO₄ + NaCl + H₂O systems.

Images were obtained every five seconds and analysed using the Process Image Analysis Expert software [28] in order to assess the crystallisation and dissolution temperatures, crystals shapes, and particle size distributions. At each rate the temperature cycle was repeated three times to obtain average values for the crystallisation and dissolution temperatures T_{cryst} and T_{diss} .

The copper sulphate system was not readily amenable to analysis via turbidometric methods due to the intense blue colour of the saturated crystallising solution [29] and hence, the determination of the metastable zone width (MSZW) [30-32] was performed using the particle viewer mode. In this, the crystallisation and dissolution temperatures were visually estimated based upon the points where the crystals appeared and disappeared, respectively (crystallisation and dissolution temperatures of the $\text{CuSO}_4 + \text{H}_2\text{O}$ and $\text{CuSO}_4 + \text{NaCl} + \text{H}_2\text{O}$ systems at different cooling rates are shown in Section S1 of the Supplementary Information (S.I.)). The resulting crystals obtained at the different cooling rates, were filtered and dried for further solid analysis (a detailed analysis of the solid-state characterisation is shown in Section S2 of the S.I.).

2.2.2 Crystal growth measurements by in-situ microscopy

In-situ crystal growth studies were carried out using an experimental set-up comprising an optical microscope (Olympus BX51) operated in Differential Interference Contrast (DIC) mode, which was integrated with a QImaging/QICAM camera which captured crystal images as a function of time. The images were then analysed using the QCapture Pro software (see:

<http://www.qimaging.com/products/software/qcappro7.php>). The associated growth cell comprised a simple temperature-controlled rectangular tank (10 x 12 cm, depth 1.5 cm) sealed with two removable rectangular glass plates. The solution was secured within a 0.5 ml sealed UV glass cuvette with a path length of 1 mm which was placed within the cell as close to the objective lens of the microscope as feasible. The temperature within the cell controlled using a Huber Ministat 125 circulating water bath that circulates water through the growth cell. The crystal growth system is shown in Figure 2.



Figure 2. Experimental set up for crystal growth rates measurements. (a) Olympus BX51 optical DIC microscope integrated with QImaging/QICAM camera. (b) Picture of the crystal growth cell.

Crystal growth experiments were performed for copper sulphate solutions (29.52 wt %) in two different media: H₂O and 2.4 wt % NaCl, where copper sulphate solutions were heated up to 70 °C to completely dissolve all crystals, after which the solutions were cooled down to a constant temperature of 23, 22, 21, 20 and 19 °C for the CuSO₄ + H₂O system, and 39, 37, 36, 35, 33 °C for CuSO₄ + NaCl + H₂O system, respectively, in order to achieve a specific supersaturation level. For each system, five different supersaturations were used. The supersaturation for crystallisation was generated by decreasing the solution temperature from the equilibrium temperature (T_e) by circulating water through the cell until the targeted

temperature had been established. The relative solution supersaturation (σ) at each temperature is calculated using equation (1).

$$\sigma = \frac{x}{x_e} - 1 \quad (1)$$

Where x is the solution concentration, and x_e is the molar fraction of the solute in the solution at equilibrium. Solubility data of copper sulphate in freshwater at different temperatures were obtained from the literature [33]. Experimental solubility data of copper sulphate with 2.4 wt % of sodium chloride at different temperatures along with the determination of activity coefficients for the assessment of ion interactions of copper sulphate in aqueous solutions and brine using the Pitzer model [14, 34-38] are shown in the Section 3 of the S.M.

The crystal morphology and growth of the observed crystals were assessed by recording images every five seconds. The growth rates of the individual faces (G) were estimated by following the increase with time of the perpendicular distance from the centre of the projected two dimensional crystal to the faces (Figure 3). The central point of the crystals was determined as the intersection points of lines connecting the crystal's corners as defined by the two most important habit faces. For each face, eleven measurements of the normal distance increase were recorded, and each experiment was performed in duplicate.

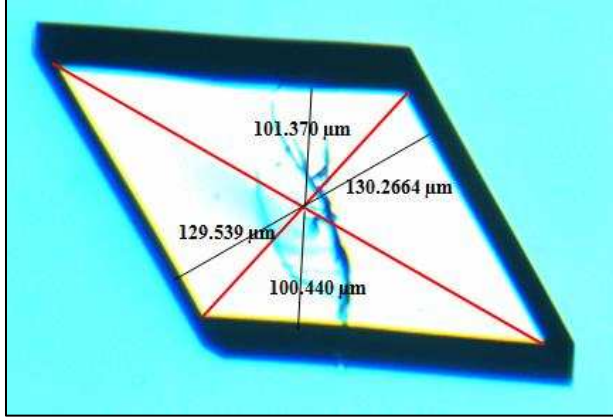


Figure 3. Example of measurement from the centre of the copper sulphate crystal to the faces. The distances are obtained by drawing a perpendicular line to each face from the centre of the crystal using QCapture Pro software.

2.2.3 Assessment of face-specific growth kinetics

The crystal growth mechanism was investigated by fitting $G(\sigma)$ dependence to models representing different interfacial crystal growth mechanisms [27], these models correspond to the Power law [39], the Birth & Spread (B&S) and Burton-Cabrera-Frank (BCF) models [40], and are given by the expressions (2), (3) and (4) respectively. A value of $r = 1$ in expression (6) corresponds to the case of Rough Interface Growth (RIG) [41].

$$G \left(\frac{m}{s} \right) = \frac{1}{\frac{1}{k_{MT}} + \frac{1}{k_G(\sigma)^{r-1}}} \sigma \quad (2)$$

$$G \left(\frac{m}{s} \right) = \frac{1}{\frac{1}{k_{MT}} + \frac{1}{k_G(\sigma)^{-1/6} \exp\left(\frac{A_1}{\sigma}\right)}} (\sigma) \quad (3)$$

$$G \left(\frac{m}{s} \right) = \frac{1}{\frac{1}{k_{MT}} + \frac{1}{k_G(\sigma) \tanh\left(\frac{A_2}{\sigma}\right)}} (\sigma) \quad (4)$$

Where k_G is the growth rate constant, r is the growth exponent in the RIG interface growth kinetic model, and A_1 and A_2 are thermodynamic parameters in the B&S and BCF interface growth kinetic models, respectively. k'_{MT} is related to the coefficient of mass transfer within the bulk of the solution, k_{MT} through expression (5).

$$k'_{MT} \left(\frac{m}{s} \right) = \frac{k_{MT} C_e MW_s}{\rho_s} \quad (5)$$

In this expression ρ_s is the solute density, MW_s the solute molecular weight and C_e the solubility.

In the expressions (2) to (4), the denominators represent the total resistance to transfer of growth units, which are given by the sum of the resistance to mass transfer within the bulk of the solution, and the resistance to incorporation of growth units at the crystal/solution interface.

In the present work, the growth kinetics of the single faces of copper sulphate pentahydrate crystals was investigated under limited conditions, as a function of media (H_2O and 2.4 wt % NaCl), and relative supersaturations, from 0.682 to 0.787 for $CuSO_4 + H_2O$ and from 0.348 to 0.458 for $CuSO_4 + NaCl + H_2O$ systems.

2.2.4 Indexing the crystal morphology

In order to confirm the Miller indices corresponding to the copper sulphate pentahydrate faces, an assessment was carried out making use of a methodology presented by Camacho et al. [26], which uses modelling routines available in Mercury 3.1. (<http://www.ccdc.cam.ac.uk/Solutions/CSDSystem/Pages/Mercury.aspx>) and HABIT [42].

This methodology relies on the prediction of the Bravais-Friedel-Donnay-Harker (BFDH) morphology using the known triclinic unit cell parameters for copper sulphate pentahydrate as given by the cif file reported by Beevers [43]. The BFDH approach relates the external shape of a crystal to the internal crystallographic lattice dimensions and symmetry and states that: “After allowing for the reduction of the growth slide thickness from space group symmetry considerations, the most morphologically important forms {hkl}, and hence those with the lowest growth rates, are those having the greatest inter-planar distance d_{hkl} ” [44].

Using the BFDH approach, d_{hkl} spacings can be taken as being inversely proportional to the perpendicular distance from the centre of the crystals to the corresponding face, which in turn can be considered as a measure of the relative growth rate for the simulation of the crystal morphology [26].

The crystal morphology was indexed by comparing the experimental morphology with predictions using the BFDH methodology.

3. Results and Discussion

3.1 On-line visualization and particle size analysis of copper sulphate crystals at different cooling rates

Figures 4 and 5, show the sequence of images of the crystallisation process as measured at four different cooling rates (from 2 to 0.3 °C/min) in two different media H₂O and 2.4 wt % NaCl.

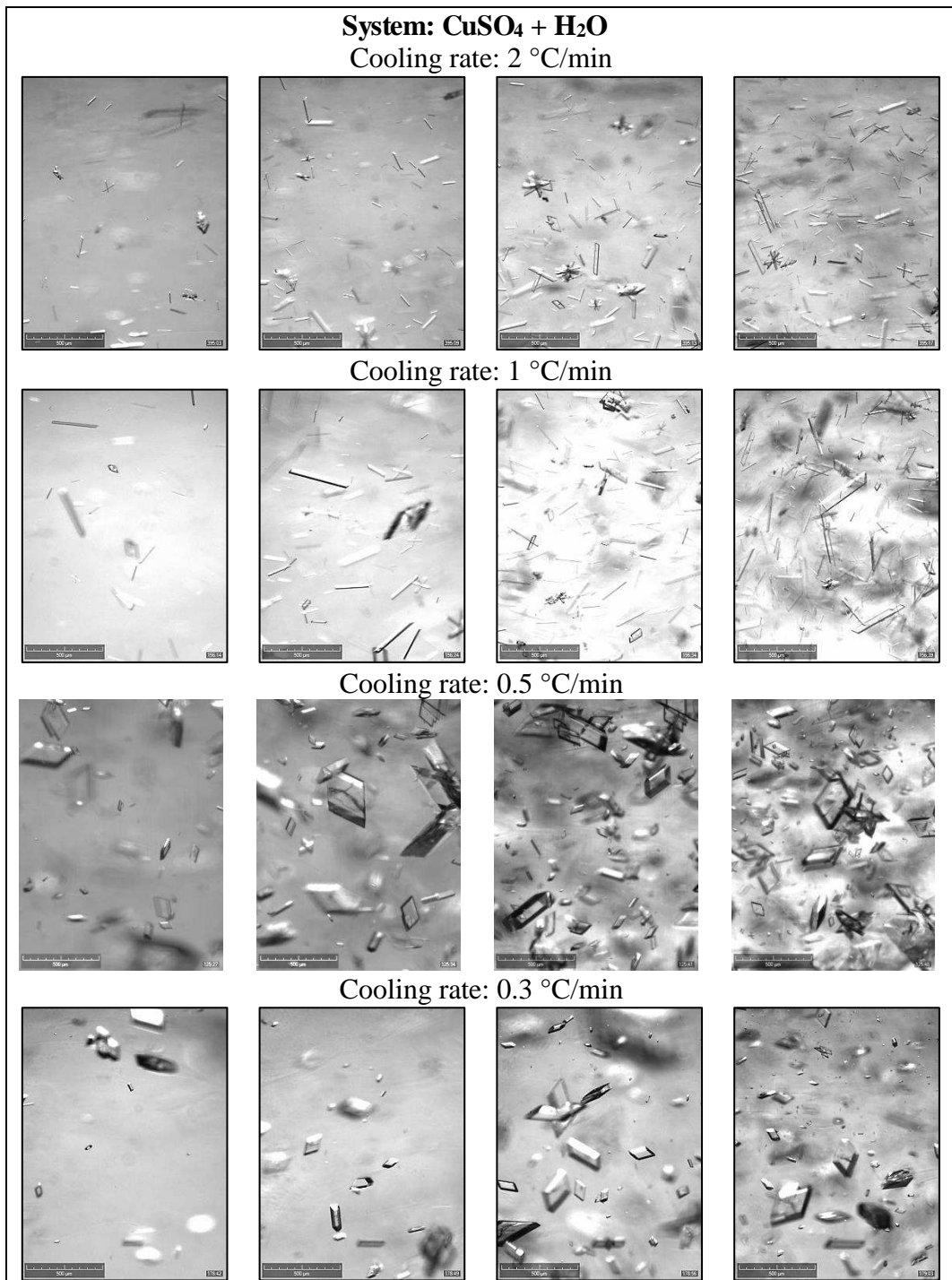


Figure 4. Sequence of pictures of copper sulphate crystals in H₂O at different cooling rates.

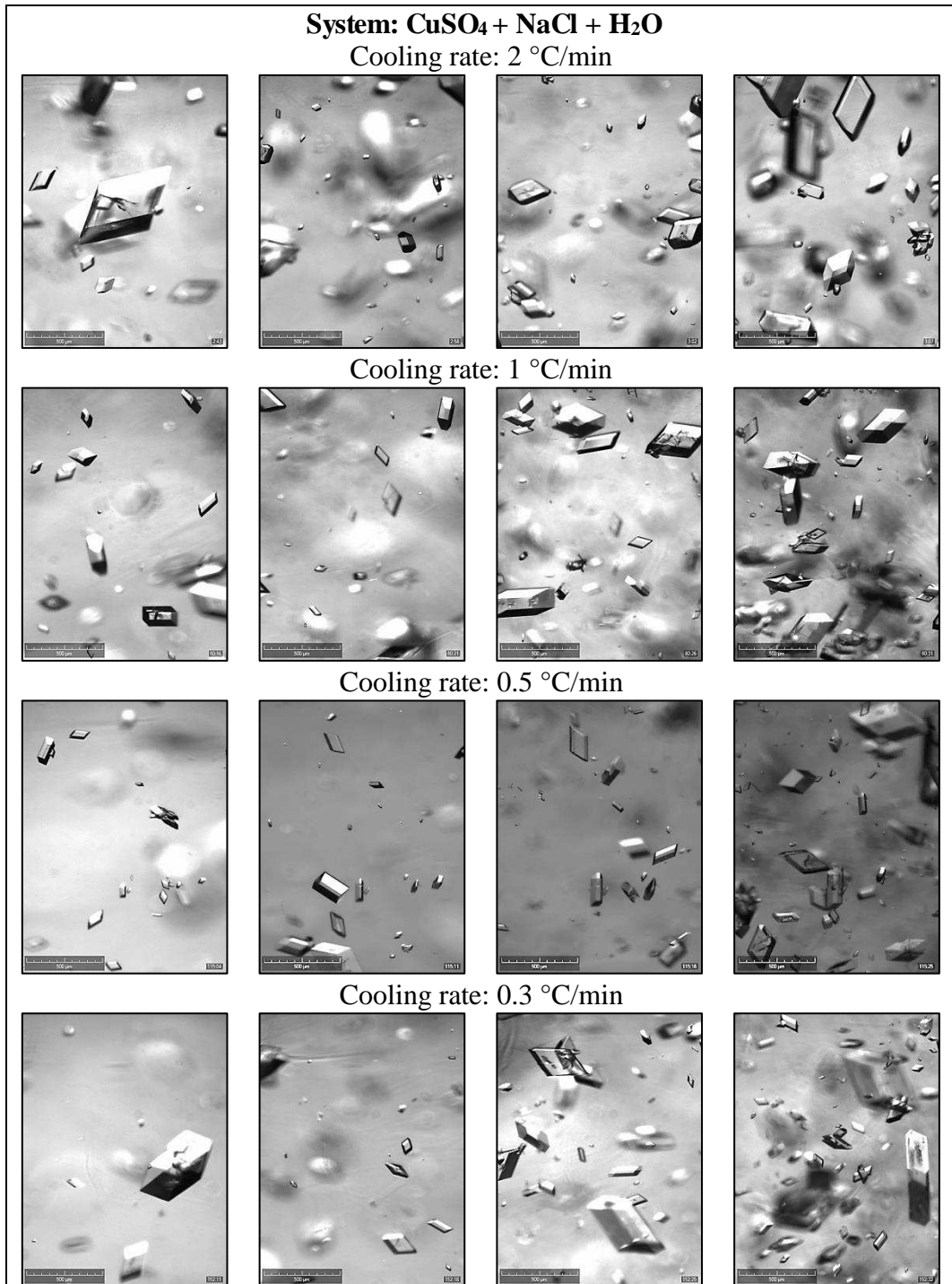


Figure 5. Sequence of pictures of copper sulphate crystals in brine at different cooling rates.

The data reveal that both the cooling rate and the sodium chloride content had a significant effect in the crystal shape, where at high cooling rates (2 and 1 °C/min) in absence of sodium chloride, copper sulphate crystals were observed to have a needle-like shape. However, at

the slower cooling rates (0.5 and 0.3 °C/min), the crystals were observed to be much more prismatic. On the other hand, when 2.4 wt % NaCl is present in the solution, crystals were also found also to be prismatic at the higher cooling rates and to maintain their shape as the cooling rate decreased.

The size range of copper sulphate crystals obtained in H₂O and 2.4 wt % NaCl media, at four different cooling rates for three different size ranges: <100 µm, <200 µm, and <300 µm, is shown in Table 1.

Table 1. Percentage copper sulphate crystals in three different size ranges at different cooling rates.

System	Size range	2 °C/min (%)	1 °C/min (%)	0.5 °C/min (%)	0.3 °C/min (%)
CuSO ₄ + H ₂ O	<100 µm	97.79	96.40	95.96	95.07
	<200 µm	2.06	3.34	3.40	4.22
	<300 µm	0.21	0.26	0.64	0.71
CuSO ₄ + NaCl + H ₂ O	<100 µm	96.03	94.56	95.08	93.15
	<200 µm	3.53	4.67	4.14	6.09
	<300 µm	0.44	0.77	0.78	0.76

Table 1 shows that there is a slight effect in the particle size when sodium chloride is present in the solution. In both systems, most of the particles are in the size range of <100 µm, and as the cooling rate decreases (from 2 to 0.3 °C/min), the presence of crystals in the ranges of < 200 and < 300 µm increases. Likewise, when copper sulphate is crystallised in brine, the percentage of particles in the higher ranges is slightly higher. Similar results have been obtained by Sheikholeslami and Ong [18] where the crystal structure and size of CaSO₄ and CaCO₃ crystals at different NaCl concentrations were studied, and was noted that as the NaCl is increased, the size of calcium sulphate and calcium carbonate increased. The larger crystal

sizes observed for the copper sulphate crystals grown in brine (Table 1) are further discussed with respect to the crystal growth kinetics in section (3.3).

3.2 Indexation of the crystal morphology of copper sulphate pentahydrate

Results from crystallisation experiments, thermal assays (TGA/DSC), and chemical analyses showed that copper sulphate crystals obtained in both H₂O and brine were found to have the same morphology and structure. The only significant differences between these crystals grown in different media was found to be the aspect ratio, which was higher for the crystals grown in pure aqueous solutions.

Due to this, the validation of the crystals faces indexation for copper sulphate pentahydrate grown in both media was carried out, based on the analysis from Beevers [43], as shown in Figure 6. This information was complemented with enlarged pictures of crystals obtained from the crystallisation data from both aqueous and brine solutions from the in process image data.

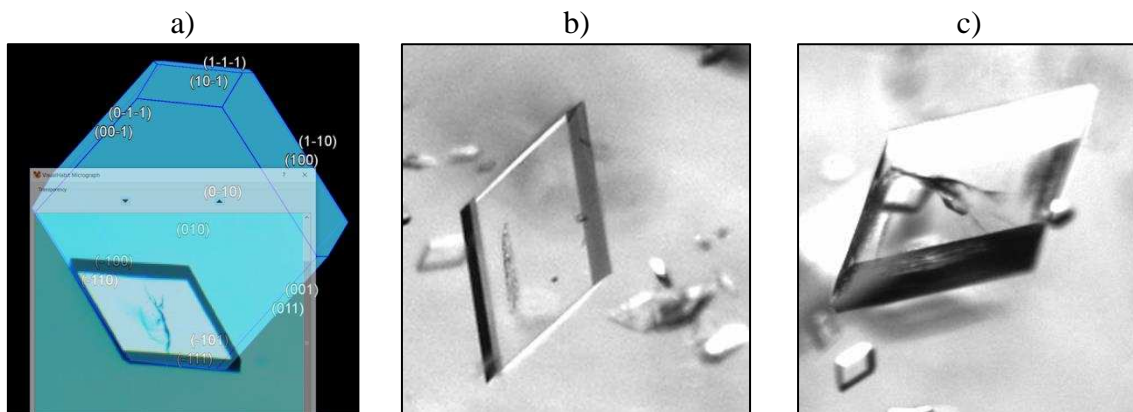


Figure 6. a) Prediction of the BFDH morphology of copper sulphate pentahydrate crystals using the Miller indices in the obtained unique solutions and comparison with the crystal micrograph obtained experimentally [45]. b) and c) Enlarged pictures of copper sulphate pentahydrate crystals obtained in aqueous solutions and brine, respectively, from Avantium Crystalline® system.

Using the methodology described in section (2.2.2), the morphological analysis revealed that the dominant faces of the copper sulphate crystal studied in this work were {1-10} and {1-1-1}, this indexation will be used through the paper to identify the faces in the growth kinetic analysis. The analysis was performed making use of the Visual Habit Tool Kit currently under development [45].

3.3 Mean growth rates and growth rates mechanism of the {1-10} and {1-1-1} faces of copper sulphate pentahydrate crystals as a function of the growth environment

A sequence of images of copper sulphate pentahydrate crystals grown in a 0.5 mL cuvette crystallisation cell in H₂O and 2.4 wt % NaCl is shown in Figure 7. The mean growth rates of the {1-10} and {1-1-1} faces of single crystals growing from H₂O and brine are presented in Table 2. The complete set of images of the crystal growth experiments is given in Section S4 in the SI.

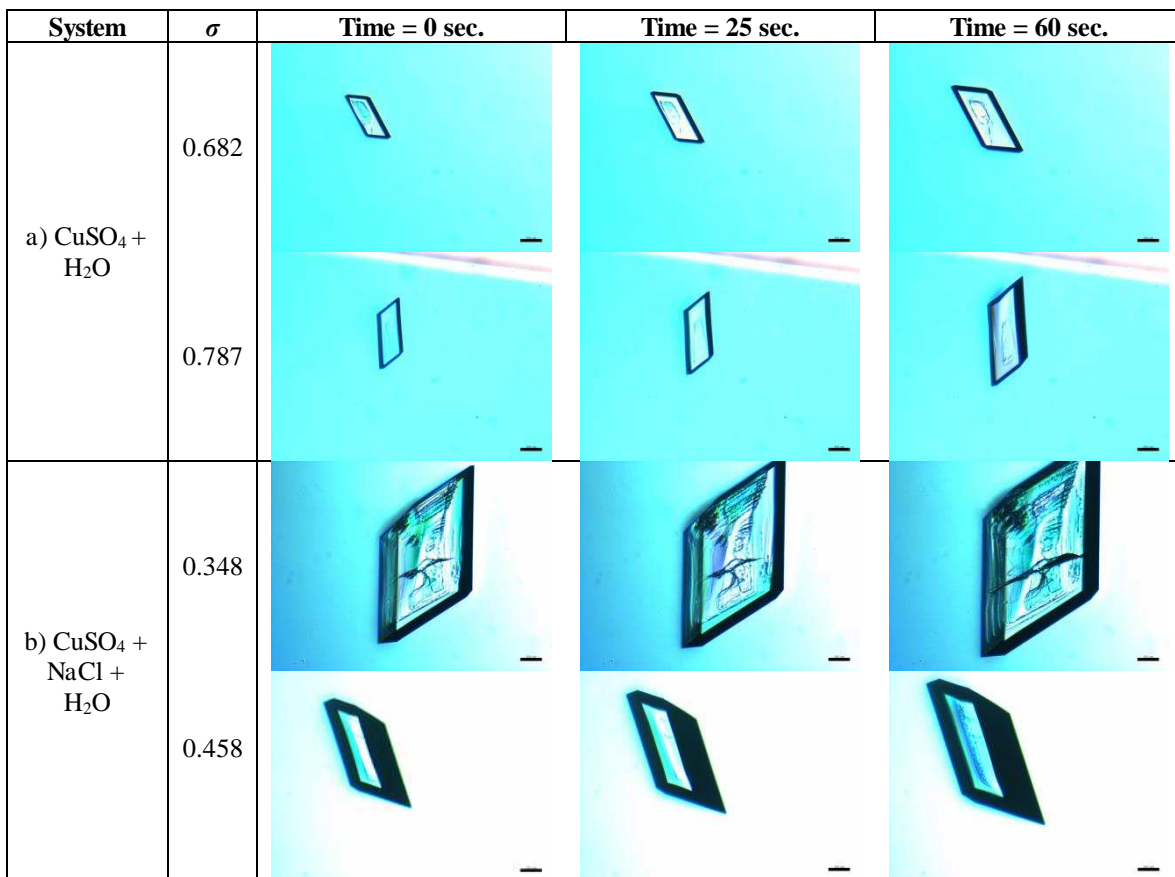


Figure 7. Series of optical micrographs of copper sulphate crystals grown in: a) H₂O at $\sigma = 0.682$ and $\sigma = 0.787$, and b) 2.4 wt % NaCl at $\sigma = 0.348$ and $\sigma = 0.458$ at the 0.5 ml scale size showing the growth of the crystals and their morphology as a function of media, elapsed time, and supersaturation. Black line in the picture represents the scale bar of 100 μm . t = 0 corresponds to the moment at which the photographs of the crystals started to be taken. This was defined as the moment in which a crystal of appropriate size was observed, to perform accurate measurements of the crystals' growth rates.

Table 2. Experimental mean growth rates of {1-10} and {1-1-1} faces of copper sulphate pentahydrate crystals growing from H₂O and 2.4 wt % NaCl media.

Solvent	σ	Number of crystals	Mean growth rate G ($\mu\text{m/sec}$)	
			{1-10}	{1-1-1}
H ₂ O	0.682	2	0.5389	0.5202
	0.708	2	0.5596	0.6124
	0.733	2	0.5855	0.6607
	0.759	2	0.5805	0.7409
	0.787	2	0.6028	0.8040
NaCl + H ₂ O	0.348	2	0.3115	0.7246
	0.383	2	0.4389	0.8555
	0.402	2	0.5026	0.9012
	0.420	2	0.5443	1.0702
	0.458	2	0.6621	1.3029

To evaluate the crystal growth mechanisms, the models described by equations (2) to (4) were fitted to the data collected for the {1-10} and {1-1-1} faces (Table 2). Given that the experimental $G(\sigma)$ observations showed that there is a critical supersaturation (σ_{crit}) below which growth does not occur (Figures 8 and 9), this parameter was introduced within the models by subtracting it from the term σ . In the present work, the quality of regression was measured by the coefficient of determination R^2 , where the fitting is considered reliable if the value of adjusted R^2 is found to be close to 100%.

Figures 8 and 9 show the best fits of these growth models to both the {1-10} and {1-1-1} faces for copper sulphate pentahydrate in H_2O and brine, respectively. Additionally, they also present the trend of the total resistance to transfer of growth units $\left(\frac{1}{K_{MTOT}}\right)$ as a function of driving force ($\Delta C = C - C_e$), using the bulk and interface transfer coefficients obtained from the experimental data fitting. $\frac{1}{K_{MTOT}}$ is defined by the denominator of the $G(\sigma)$ expressions given by the corresponding mechanistic model assessed.

Table 3 shows the obtained parameters for the growth models that best fit the experimental data, and the corresponding R^2 values for both {1-10} and {1-1-1} faces. Here, when more than one model fitted well to the experimental data the corresponding modelled parameters are all given. In addition to this, an estimation of both the resistance to transfer within the bulk and that at the interface are given in Table 3 using average values of σ and C_e within the range of study.

The fitting to the experimental data of all the mechanistic models including: power law, B&S and BCF is given in Section S5 of the S.I.

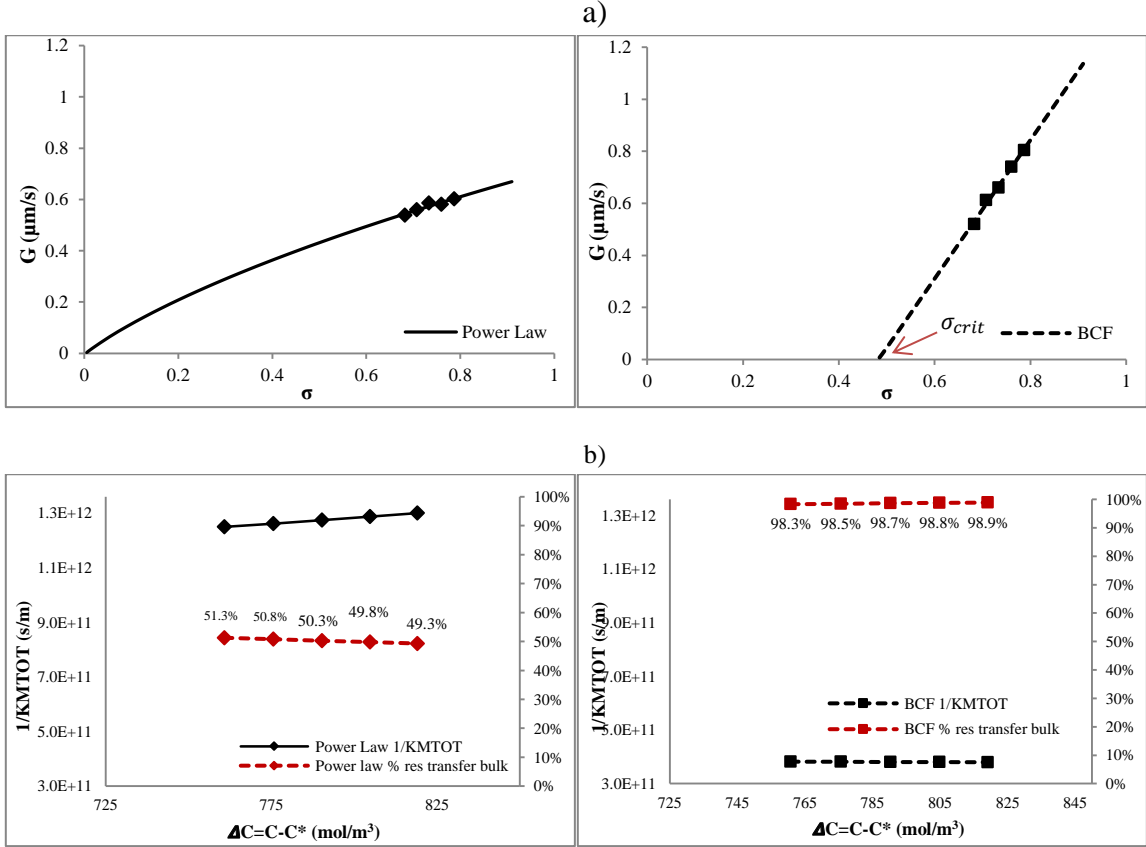


Figure 8. Copper sulphate crystals growing from H_2O media. For each set of four plots, a) $G(\sigma)$ experimental data fitted to the Power law and BCF models; b) trend of the total resistance to mass transfer as a function of ΔC using the parameters obtained from the data fitting to these models. The dotted red line shows the trend of the ratio of the resistance to mass transfer in the bulk to the total resistance. Left (♦) refers to the {1-10} and right (■) to the {1-1-1} faces respectively.

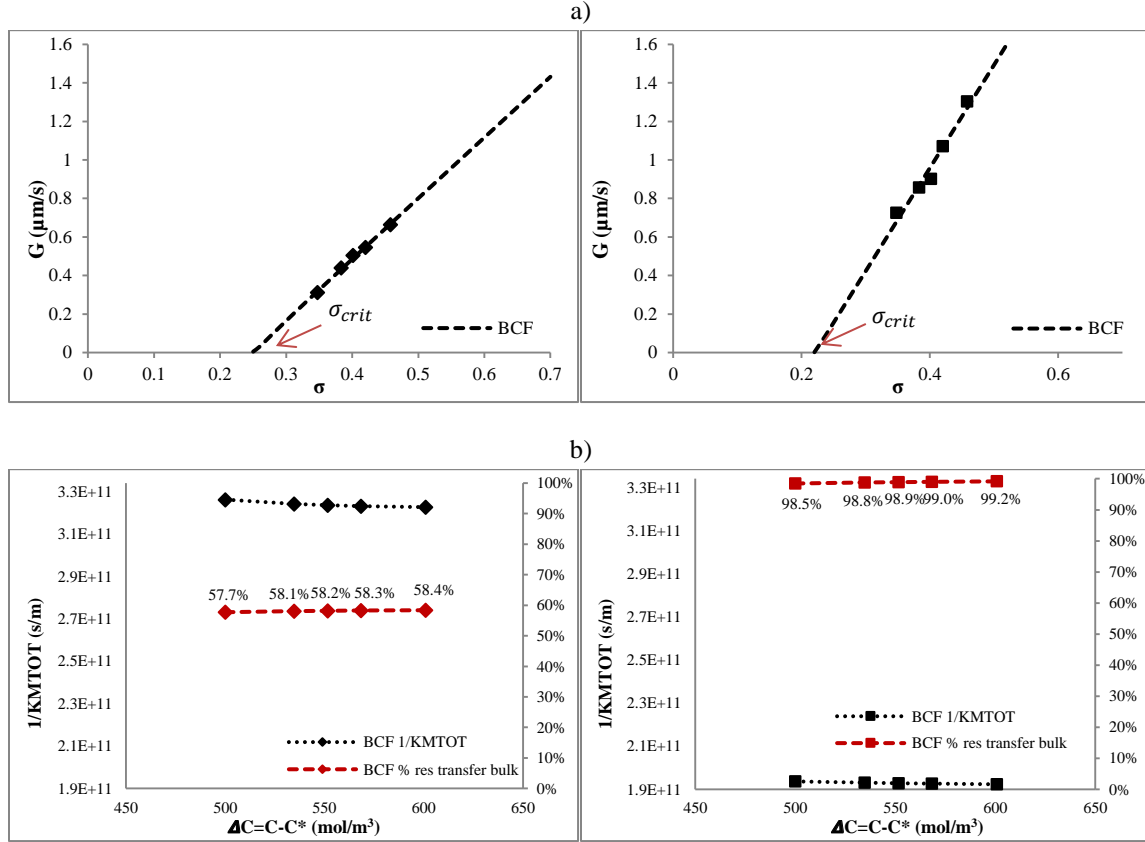


Figure 9. Copper sulphate crystals growing from 2.4 wt % NaCl media. For each set of four plots, a) $G(\sigma)$ experimental data fitted to the BCF model; b) trend of the total resistance to mass transfer as a function of ΔC using the parameters obtained from the data fitting to these models. The dotted red line shows the trend of the ratio of the resistance to mass transfer in the bulk to the total resistance. Left (\blacklozenge) refers to the {1-10} and right (\blacksquare) to the {1-1-1} faces, respectively.

Figures 8 and 9 show that regardless the media in where the copper sulphate pentahydrate crystal were grown, as expected, when the driving force increases (supersaturation) the crystal growth rate increases for both crystal faces. However, depending on the kinetic mechanism associated to each of the faces, the degree of change on the growth rate related to the supersaturation will vary. In addition to this is clear from these Figures that the growth rate of the {1-1-1} face is always higher than that of the {1-10}, which results in elongated crystals on the direction of the {1-1-1} face.

For crystals grown in pure aqueous solutions, the results suggest that for the {1-10} face, the best fitting to the experimental data was obtained for the power law model for which a R^2 value of 90% was obtained, delivering a σ_{crit} value of 0.003. These results imply that the growth in this case occurs continuously, practically at any supersaturation level. On the other hand, for the {1-1-1} face, the best fitting to the experimental data was obtained for the BCF mechanistic model. This conclusion is strengthened by the fact that for the fitting through the power law a value of 1.09 was obtained for the parameter r. At high supersaturation levels, such as those used in this analysis, a value of r equal to one is correlated with the BCF mechanism [46].

For crystals grown in brine, the best fitting to the experimental data was obtained for the BCF mechanistic model for both the {1-10} and {1-1-1} faces. Similarly to the case of crystallisation from aqueous solutions, the r values obtained through the fitting of the data to a power law delivered 0.99 and 1.03 respectively for the parameter r, which supports the case for growth though the BCF mechanism [46].

Table 3. Crystal growth kinetics parameters obtained from the best fit of the models given by the equations (6) and (8) to the experimental $G(\sigma)$ data.

		CuSO ₄ + H ₂ O		CuSO ₄ + NaCl + H ₂ O	
	Range σ studied	0.682 to 0.787		0.348 to 0.458	
Fitting model	Range of $\Delta C = (C - C_e)$ studied	760.8 to 819.1		500.1 to 600.9	
Power law Equation (6)	Faces	{1-10}	{1-1-1}	{1-10}	{1-1-1}
	$\frac{1}{k_{MT}}$	6.40E+11	3.31E+11	4.74E+10	4.75E+10
	$k_{MT} \left(\frac{m}{s} \right)$	1.75E-11	3.38E-11	1.83E-10	1.82E-10
	$k_G \left(\frac{m}{s} \right)$	1.33E+00	2.29E+01	3.66E-12	7.48E-12
	$\frac{1}{k_G(\sigma - \sigma_{crit})^{r-1}}$	6.34E-01	4.92E-02	2.72E+11	1.41E+11
	σ_{crit}	0.003	0.480	0.245	0.219
	r	0.45	1.09	0.9983	1.0331
	R^2	90%	99%	99%	96%
BCF Equation (8)	$\frac{1}{k_{MT}}$		3.75E+11	1.86E+11	1.87E+11
	$k_{MT} \left(\frac{m}{s} \right)$		2.98E-11	4.65E-11	4.63E-11
	$k_G \left(\frac{m}{s} \right)$		7.68E+02	2.27E-10	2.70E-09
	$\frac{1}{k_G(\sigma - \sigma_{crit}) \tanh \left(\frac{A_2}{(\sigma - \sigma_{crit})} \right)}$		5.13E-03	1.32E+11	7.19E+08
	σ_{crit}		0.480	0.245	0.219
	A_2		9.507	0.034	47.660
	R^2		99%	99.5%	96%
Rate limiting step		Diffusion of growth units within the bulk of the solution		Diffusion of growth units within the bulk of the solution	

Whilst the amount of experimental data collected is probably not enough to accurately determine the values of k_{MT} and k_G the fitting of the models presented to these data, can deliver relevant mechanistic information through the comparison between the resistance to mass transfer within the bulk of the solution and that of the resistance to incorporation of growth units at the crystal/solution interface.

For the case of aqueous solutions, it was found that for both the {1-10} and {1-1-1} faces the resistance to mass transfer is twelve and fourteen orders of magnitude higher, respectively,

than the resistance to incorporation of growth units at the interface. This means that the diffusion of growth units within the bulk of the solution is the rate limiting step. This conclusion is also supported by Figure 8b which shows that the resistance to mass transfer is between 49.3% and 51.3% of the total resistance to growth for the {1-10} face, and between 98.3 and 98.9% for the {1-1-1} face. In addition to this, the growth rate pre-exponential term k_G is two orders of magnitude higher for the {1-1-1} face. Thus the molecular integration to this face is higher which explains that these crystals have a more elongated habit in this direction at the studied supersaturation range.

For crystals grown in brine, the resistance to mass transfer is of equal order of magnitude to that at the interface for the {1-10} face while for the {1-1-1} face, is three orders of magnitude higher. This suggests that the latter face will grow the fastest, as there is higher speed of molecular integration to this face which results in slightly elongated crystals perpendicular to this direction. Similarly, to the case of growth from aqueous solutions the resistance to mass transfer is between 57.7% and 58.4% of the total resistance to growth for the {1-10} face, and between 98.5 and 99.2% for the {1-1-1} face confirming that in all cases the transfer of growth units within the bulk of the solution is the rate limiting step.

The results obtained from the growth kinetic analysis are in agreement with those results shown in Figure 7, where it is observed that at high and low supersaturations, crystals grown in H₂O media are slightly more elongated than those in brine. These results could reflect the different surface chemistry of the habit faces and hence the different interface kinetic mechanisms that might govern the growth of each face in the case of H₂O media. However, in brine the growth might be ruled by the presence of screw dislocations in both faces in

agreement with a BCF mechanistic model. In addition, a comparison of the k_G values reveals that they are higher in H₂O media while differing between the two faces by two orders of magnitude in the case of H₂O media compared to just one order of magnitude in the case of brine. This, makes the integration of growth units a slower and more balanced process in the latter case delivering more prismatic crystals.

With the aim of comparing the influence of the sodium chloride on the growth rates of {1-10} and {1-1-1} faces, an extrapolation of the growth rate data was performed using Equations (2) and (4), and the results are shown in Figure 10.

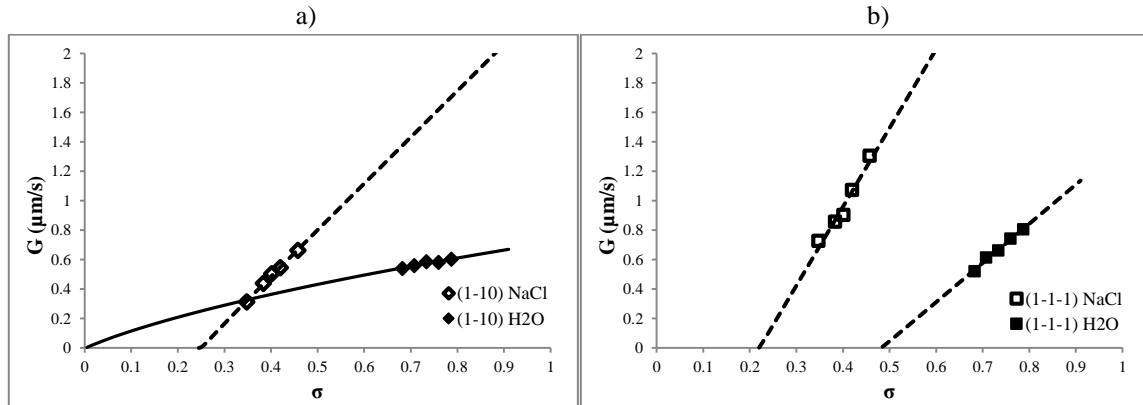


Figure 10. Sodium chloride effect in the a) {1-10} and b) {1-1-1} crystal faces of copper sulphate pentahydrate. Extrapolated data are given by the black and dotted lines representing the best fit of the data through the Power law and BCF models, respectively.

This comparison suggests that for both the {1-10} and {1-1-1} faces, the growth rates in brine are generally higher than in H₂O media which is in agreement with previous studies on the growth kinetics of related compounds, such as gypsum growing from H₂O and NaCl (Brandse et al. [17]), which have shown that the addition of sodium chloride accelerates the growth rates remarkably.

Summarizing, the increment in size of copper sulphate crystals when sodium chloride is present in the solution is mainly attributed to the higher growth rate of the crystal faces when crystals are grown in brine.

4. Conclusions

The influence of solution cooling rate and sodium chloride addition on the crystal morphology, size, composition, and growth rates of copper sulphate pentahydrate crystals has been examined in order to evaluate the impact on crystal form, of using seawater as an alternative to pure water, for the industrial process associated with copper sulphate pentahydrate crystallisation.

Higher cooling rates and/or the addition of sodium chloride were found to have a relevant effect in the shape of copper sulphate pentahydrate crystals, where the habit was found to change from an acicular shape, when crystals are in pure aqueous media, to prismatic crystals in the presence of NaCl. The percentage of particles in higher size ranges was slightly increased in brine.

In general, this study suggests that crystals grown in brine are larger compared to those grown in pure aqueous solutions. This behaviour can be mainly attributed to differences in the growth kinetics due to the presence of NaCl, which can even induce a mechanistic change particularly in the case of the {1-10} face, where a change in the growth mechanism is observed. In order to obtain a deeper understanding of the effect of NaCl in the crystallisation of copper sulphate pentahydrate, it would be interesting to use molecular and synthonic

modelling techniques [45] to carry out a chemical interaction analysis between the solution species and the specific habit faces of the crystals.

Acknowledgements: Francisca Justel acknowledges the EPSRC Centre for Doctoral Training in Complex Particulate Products and Processes (grant reference EP/L015285/1) for the support in this research which was carried out at the University of Leeds as part of her doctoral studies [47], and CONICYT, Chile for providing the Ph.D. scholarship. The authors also gratefully acknowledge the UK's EPSRC for the support of nucleation and crystal growth research at Leeds and Manchester through funding the Critical Mass Project: Molecules, Clusters and Crystals (Grant references EP/IO14446/1 and EP/IO13563/1).

List of Symbols

α Constant of the Pitzer model

A_\varnothing Debye-Hückel constant for the osmotic coefficients in the Pitzer model

A_1 Growth parameter in B&S model

A_2 Growth parameter in the BCF model

b Constant of the Pitzer model

$\beta^{(0)}, \beta^{(1)}, \beta^{(2)}, C^\varnothing$ Solute-specific interaction parameters of the Pitzer model

b Dimensionless thermodynamic parameter

C_e Equilibrium concentration (m^{-3})

d_{hkl} Inter-planar distances within morphological (hkl) forms

$f^\gamma, B^\gamma, C^\gamma$ Ion-interaction parameters of the Pitzer model

G Single face growth rate ($m s^{-1}$)

I Ionic strength

k_G Growth rate constant ($m^{\left(\frac{1}{m}\right)} s^{-1}$)

k_{MT} Mass transfer coefficient ($m s^{-1}$)

m Molality

r Growth exponent

T Solution temperature (K)

T_{cryst} Crystallisation temperature (K)

T_{diss} Equilibrium dissolution temperature (K)

x Mole fraction of solute in solution

x_e Equilibrium mole fraction

σ Relative supersaturation

σ_{crit} Critical relative supersaturation

γ_{\pm} Activity coefficient

ρ Density

List of Abbreviations

BCF Burton-Cabrera-Frank model

BFDH Bravais-Friedel-Donnay-Harker model

B&S Birth and Spread model

Cif Crystallographic information file

$MSZW$ Metastable zone width

MW Molecular weight

RIG Rough Interface Growth model

SD Standard deviation

$2D$ Two dimensional

SI Supplementary information

References

- [1] M. Giulietti, S. Derenzo, J. Nývt, L. Ishida, Crystallization of copper sulphate, *Crystal Research and Technology*, 30 (1995) 177-183.
- [2] S. Aktas, A novel purification method for copper sulfate using ethanol, *Hydrometallurgy*, 106 (2011) 175-178.
- [3] H.W. Richardson, *Handbook of copper compounds and applications*, CRC Press, 1997.
- [4] M.E. Schlesinger, M.J. King, K.C. Sole, W.G. Davenport, *Extractive metallurgy of copper*, Elsevier, 2011.
- [5] L.A. Cisternas, L. Moreno, *El agua de mar en la minería: Fundamentos y aplicaciones*, in, RIL editores, 2014, pp. 234.
- [6] V. Manomenova, M. Stepnova, V. Grebenev, E. Rudneva, A. Voloshin, Growth of CuSO₄· 5H₂O single crystals and study of some of their properties, *Crystallography Reports*, 58 (2013) 513-516.
- [7] T. Ishii, S. Fujita, Crystallization from supersaturated cupric sulfate solutions in a batchwise stirred tank, *The Chemical Engineering Journal*, 21 (1981) 255-260.
- [8] R.C. Zumstein, R.W. Rousseau, Agglomeration of copper sulfate pentahydrate crystals within well-mixed crystallizers, *Chemical engineering science*, 44 (1989) 2149-2155.
- [9] M. Giulietti, M. Seckler, S. Derenzo, J. Valarelli, Changes in copper sulfate crystal habit during cooling crystallization, *Journal of crystal growth*, 166 (1996) 1089-1093.
- [10] M. Giulietti, M. Seckler, S. Derenzo, L. Schiavon, J. Valarelli, J. Nyvt, Effect of selected parameters on crystallization of copper sulphate pentahydrate, *Crystal Research and Technology*, 34 (1999) 959-967.
- [11] P.a.C. Hernández, H.c.R. Galleguillos, T.f.A. Gruber, E.K. Flores, M.E. Taboada, Effect of Seawater on the Solubility and Physicochemical Properties of Acidic Copper Sulfate Solutions, *Journal of Chemical & Engineering Data*, 57 (2012) 2430-2436.
- [12] F. Justel, M. Claros, M. Taboada, Solubilities and physical properties of saturated solutions in the copper sulfate + sulfuric acid + seawater system at different temperatures, *Brazilian Journal of Chemical Engineering*, 32 (2015) 629-635.
- [13] F.J. Justel, M.E. Taboada, Y.P. Jimenez, Solid–liquid equilibrium and copper sulfate crystallization process design from a sulfuric-acid–seawater system in the temperature range from 293.15 to 333.15 K, *Industrial & Engineering Chemistry Research*, 56 (2017) 4477-4487.

- [14] F.J. Justel, M.E. Taboada, Y.P. Jiménez, Thermodynamic study of the Cu-Na-H-SO₄-Cl-HSO₄-H₂O system for the solubility of copper sulfate in acid seawater at different temperatures, *Journal of Molecular Liquids*, 249 (2017) 702-709.
- [15] A.T. Kan, G. Fu, M.B. Tomson, Effect of methanol and ethylene glycol on sulfates and halite scale formation, *Industrial & Engineering Chemistry Research*, 42 (2003) 2399-2408.
- [16] Y.P. Jimenez, M.E. Taboada, H.R. Galleguillos, Solid-liquid equilibrium of K₂SO₄ in solvent mixtures at different temperatures, *Fluid Phase Equilibria*, 284 (2009) 114-117.
- [17] W. Brandse, G. Van Rosmalen, G. Brouwer, The influence of sodium chloride on the crystallization rate of gypsum, *Journal of Inorganic and Nuclear Chemistry*, 39 (1977) 2007-2010.
- [18] R. Sheikholeslami, H. Ong, Kinetics and thermodynamics of calcium carbonate and calcium sulfate at salinities up to 1.5 M, *Desalination*, 157 (2003) 217-234.
- [19] J. Garside, A. Mersmann, J. Nývlt, Measurement of crystal growth and nucleation rates, IChemE, 2002.
- [20] T.T.H. Nguyen, Influence of crystallisation environment on the nucleation and growth of single crystals of (RS)-ibuprofen, University of Leeds, 2013.
- [21] J. Mullin, A. Amatavivadhana, Growth kinetics of ammonium and potassium dihydrogen phosphate crystals, *Journal of Chemical Technology and Biotechnology*, 17 (1967) 151-156.
- [22] R. Davey, J. Mullin, Growth of the {101} faces of ammonium dihydrogen phosphate crystals in the presence of ionic species, *Journal of crystal growth*, 23 (1974) 89-94.
- [23] C. Sweegers, H. Meekes, W. Van Enckevort, I. Hiralal, A. Rijkeboer, Growth rate analysis of gibbsite single crystals growing from aqueous sodium aluminate solutions, *Crystal Growth & Design*, 4 (2004) 185-198.
- [24] S. Suharso, In Situ Measurement of the Growth Rate of the (111) Face of Borax Single Crystal, *Jurnal Matematika & Sains*, 10 (2009) 101-106.
- [25] T. Nguyen, R. Hammond, K. Roberts, I. Marziano, G. Nichols, Precision measurement of the growth rate and mechanism of ibuprofen {001} and {011} as a function of crystallization environment, *CrystEngComm*, 16 (2014) 4568-4586.
- [26] D.M. Camacho, K.J. Roberts, K. Lewtas, I. More, The crystal morphology and growth rates of triclinic N-docosane crystallising from N-dodecane solutions, *Journal of crystal growth*, 416 (2015) 47-56.

- [27] D.M. Camacho, K.J. Roberts, F. Muller, D. Thomas, I. More, K. Lewtas, Morphology and growth of methyl stearate as a function of crystallisation environment, *Crystal Growth & Design*, (2016).
- [28] X.Z.r.g. Wang, Process Image Analysis Expert software developed at University of Leeds, in, 2010.
- [29] E. Lyall, P. Mougin, D. Wilkinson, K.J. Roberts, In situ ultrasonic spectroscopy study of the nucleation and growth of copper sulfate pentahydrate batch crystallized from supersaturated aqueous solutions, *Industrial & Engineering Chemistry Research*, 43 (2004) 4947-4956.
- [30] J. Ulrich, C. Stuge, Some aspects of the importance of metastable zone width and nucleation in industrial crystallizers, *Journal of crystal growth*, 237 (2002) 2130-2135.
- [31] N. Kubota, A new interpretation of metastable zone widths measured for unseeded solutions, *Journal of crystal growth*, 310 (2008) 629-634.
- [32] D. Kashchiev, A. Borissova, R.B. Hammond, K.J. Roberts, Effect of cooling rate on the critical undercooling for crystallization, *Journal of crystal growth*, 312 (2010) 698-704.
- [33] W.F. Linke, A. Seidell, Solubilities, inorganic and metal-organic compounds: a compilation of solubility data from the periodical literature, American Chemical Society Washington, DC, 1958.
- [34] N. Rajarao, V. Brahmajirao, A. Sarma, Studies on Ion-Solvent Interactions of Electrolyte Solutions—Part 3: Activity Coefficient Studies of 2-2 Electrolytes (Sulphates of Transition Metals), *International Journal of Science and Technology*, 1 (2012).
- [35] K.S. Pitzer, G. Mayorga, Thermodynamics of electrolytes. III. Activity and osmotic coefficients for 2–2 electrolytes, *Journal of Solution Chemistry*, 3 (1974) 539-546.
- [36] S. Clegg, M. Whitfield, Activity coefficients in natural waters, *Activity coefficients in electrolyte solutions*, 2 (1991).
- [37] J.O.M. Bockris, A.K.N. Reddy, *Modern Electrochemistry*, in: N.Y. Reverté (Ed.), 1979.
- [38] J.W. Morales Saavedra, Tesis Doctoral: Estudio Termodinámico de sistemas ternarios Sal + PEG 4000 + Agua a las temperaturas de (288.15, 298.15 y 308.15) K, in, 2011.
- [39] J. Garside, Industrial crystallization from solution, *Chemical engineering science*, 40 (1985) 3-26.

- [40] W.-K. Burton, N. Cabrera, F. Frank, The growth of crystals and the equilibrium structure of their surfaces, Philosophical Transactions of the Royal Society of London A: Mathematical, Physical and Engineering Sciences, 243 (1951) 299-358.
- [41] J.D. Weeks, G.H. Gilmer, Dynamics of crystal growth, Adv. Chem. Phys, 40 (1979) 157-227.
- [42] G. Clydesdale, R. Docherty, K. Roberts, HABIT-a program for predicting the morphology of molecular crystals, Computer Physics Communications, 64 (1991) 311-328.
- [43] C. Beevers, H. Lipson, The Crystal Structure of Copper Sulphate Pentahydrate, CuSO₄*5H₂O, Proceedings of the Royal Society of London. Series A, 146 (1934) 570-582.
- [44] J.D.H. Donnay, D. Harker, A new law of crystal morphology extending the law of Bravais, Am. Mineral, 22 (1937) 446-467.
- [45] R.B.H. J Pickering, V Ramachandran, M Soufian and K J Roberts, Synthonic Engineering Modelling Tools for Product and Process Design, Chapter 10 In: Engineering Crystallography: From Molecule to Crystal to Functional Form (edited by K J Roberts, R Docherty R and R Tamura) in: S.S.B. Media (Ed.), 2017.
- [46] J.W. Mullin, Crystallization, Butterworth-Heinemann, 2001.
- [47] F.J. Justel, Thesis: The effect of seawater on the thermodynamics and crystallization of copper sulfate pentahydrate, in: Departamento de Ingeniería Química y Procesos de Minerales, Universidad de Antofagasta, Antofagasta, 2017.